REPORT DOCUMENTATION PAGE

Form Approved
OMB No. 0704-0188

1. AGENCY USE ONLY *(Leave blank)*	2. REPORT DATE	3. REPORT TYPE AND DATES COVERED
	August 2002	Technical Report

4. TITLE AND SUBTITLE
ASSESSMENT OF CARDIOVASCULAR DYNAMICS USING PERIODICITY ATTRIBUTES DERIVED FROM PERIPHERAL BLOOD FLOW SIGNALS

5. FUNDING NUMBERS

6. AUTHOR(S)
Partha P. Kanjilal, Ph.D. and Richard R. Gonzalez, Ph.D.

7. PERFORMING ORGANIZATION NAME(S) AND ADDRESS(ES)
U.S. Army Research Institute of Environmental Medicine
Kansas St, BLDG 42
NATICK, MA 01770-5007

8. PERFORMING ORGANIZATION REPORT NUMBER
T02-17

9. SPONSORING / MONITORING AGENCY NAME(S) AND ADDRESS(ES)
U.S. Army Medical Research and Materiel Command
Fort Detrick, MD 01760-5007

10. SPONSORING / MONITORING AGENCY REPORT NUMBER

11. SUPPLEMENTARY NOTES

12a. DISTRIBUTION / AVAILABILITY STATEMENT
Approved for public release; distribution unlimited

12b. DISTRIBUTION CODE

13. ABSTRACT *(Maximum 200 words)*

A periodic process can be characterized in terms of three periodicity (or p-) attributes: the periodicity (or period-length), the periodic wave-shape or pattern and the wave-magnitude or the scaling factor; all three attributes can be time varying in a real-life situation. In this report, we hypothesize that an analysis of the dynamics underlying a nearly periodic physiological process, such as appearing in a rhythmic blood wave pattern, can be quantified in terms of the dynamics of its periodicity attributes. This report analyzes data obtained from archival studies in which the photo-plethysmograph signal (PPS) is recorded from the finger. Each specific blood wave signal is decomposed into a regular component, which is nearly periodic, and an irregular residual process. The dynamics of the PPS p-attributes of the regular part are analyzed individually as well as collectively to assess the general cardiovascular state. A new class of surrogate series based on the shuffling of the p-attributes is proposed to detect the nonlinear determinism in the PPS. The dynamics is further studied by mapping the variations of the p-attributes in a novel p-space, defined by the three orthogonal periodicity-attribute components; each point in the p-space represents one nearly periodic segment. Novel complexity measures based on global and temporal variations of dynamics in the p-space are proposed. A correlation is explored between the complexity measures derived from the p-space mapping of PPS that closely matches the cardiovascular state of a typical human subject.
The mathematical algorithms derived from a simple blood flow wave pattern can be easily applied for assessing other physiologic signals in the cardiovascular system obtained during perturbations caused by dynamic exercise, thermal stress, and potentially high terrestrial physiologic effects during hypobaric stress.

14. SUBJECT TERMS
modeling, cardiovascular dynamics, plethysmography, orthogonal transformation, periodic process, nonlinear dynamics, chaos, time series, WPSM signal processing

15. NUMBER OF PAGES
23

16. PRICE CODE

17. SECURITY CLASSIFICATION OF REPORT	18. SECURITY CLASSIFICATION OF THIS PAGE	19. SECURITY CLASSIFICATION OF ABSTRACT	20. LIMITATION OF ABSTRACT
U	U	U	NONE

U.S. ARMY RESEARCH INSTITUTE OF ENVIRONMENTAL MEDICINE

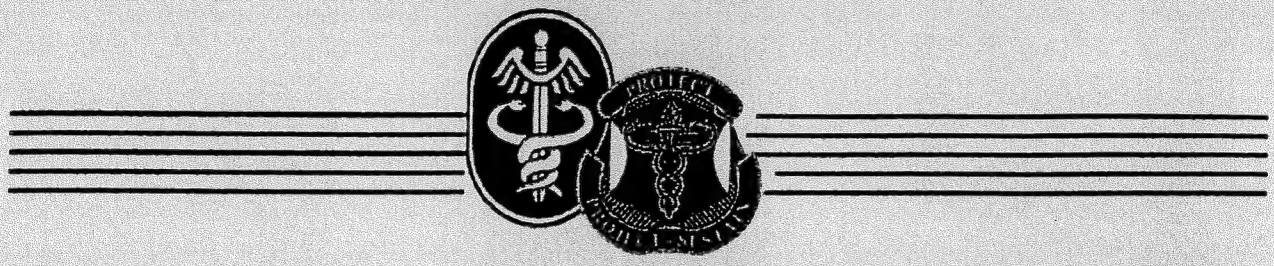

TECHNICAL REPORT NO. T-02/17
DATE August 2002
AD A402997

ASSESSMENT OF CARDIOVASCULAR DYNAMICS USING PERIODICITY ATTRIBUTES DERIVED FROM PERIPHERAL BLOOD FLOW SIGNALS

U.S. ARMY MEDICAL RESEARCH AND MATERIEL COMMAND

Disclaimer

DTIC AVAILABILITY NOTICE

USARIEM TECHNICAL REPORT T02/17

ASSESSMENT OF CARDIOVASCULAR DYNAMICS USING PERIODICITY ATTRIBUTES DERIVED FROM PERIPHERAL BLOOD FLOW SIGNALS

Partha P. Kanjilal, Ph.D.

Richard R. Gonzalez, Ph.D.

Biophysics and Biomedical Modeling Division

August 2002

U.S. Army Research Institute of Environmental Medicine
Natick, MA 01760-5007

TABLE OF CONTENTS

Section	Page
List of Figures	iv
List of Tables	v
Executive Summary	1
Introduction	2
Methods	3
Results	5
Assessment of nonlinearity using surrogate data	5
Proposed surrogates	7
Generation of surrogates	7
Detection of determination	8
Proposed p-attribute map and complexity measures	9
Characterization of dynamics through p-attribute space distribution	9
Case study analyses	10
p-map dynamics	16
Conclusions	17
References	18

LIST OF FIGURES

Figure		Page
1	(a) The variations in the periodicity over a segment of data in Case-2, (b) the corresponding variations of the scaling factor, (c) the varying pattern profiles of the successive periodic segments with the periodic length defaulted to a fixed value	12
2	(a)-(b) The photo-plethysmograph signal for a post-operative stable patient (case-1 in Table 1), and its phase-space plot. (c)-(d) the regular component extracted from the signal (a), and the corresponding phase-space plot. (e)-(f) the AAFT surrogate series generated from (c), and the corresponding phase-space plot. (g)-(h) the surrogate generated by shuffling the scaling factors and corresponding phase-space plot. (i)-(j) the surrogate generated by shuffling the patterns of the periodic segments and the corresponding phase-space plot. Note that in both (h) and (j) the noisy limit cycle structure is retained, whereas in (f) it is destroyed.	13
3	Column (a): The scaled singular value distribution of the regular component against the same for the surrogates generated through the shuffling of the periodicity, the pattern, and the scaling sequences for Cases-1 to Case-6. Column (b): the scaled singular value distribution of the residual component against the AAFT surrogated for Case-1 to Case-6. Column (c): Profiles of the distances between successive points in the p-map for Case-1 to Case-6.	14
4	Fraction of points in successive shells centered around the reference point in the p-map for Case-1 to Case-6	15

LIST OF TABLES

Table		Page
1	Summary of case studies from archival database [10]	11

EXECUTIVE SUMMARY

A periodic process can be characterized in terms of three periodicity (or *p*-) attributes: the periodicity (or period-length), the periodic wave-shape or pattern and the wave-magnitude or the scaling factor; all three attributes can be time varying in a real-life situation.

In this report, we hypothesize that an analysis of the dynamics underlying a nearly periodic physiological process, such as appearing in a rhythmic blood wave pattern, can be quantified in terms of the dynamics of its periodicity attributes. This report analyzes data obtained from archival studies in which the photo-plethysmograph signal (PPS) is recorded from the finger. Each specific blood wave signal is decomposed into a regular component, which is nearly periodic, and an irregular residual process. The dynamics of the PPS *p*-attributes of the regular part are analyzed individually as well as collectively to assess the general cardiovascular state.

A new class of surrogate series based on the shuffling of the *p*-attributes is proposed to detect the nonlinear determinism in the PPS. The dynamics is further studied by mapping the variations of the *p*-attributes in a novel *p-space*, defined by the three orthogonal periodicity-attribute components; each point in the *p*-space represents one nearly periodic segment. Novel complexity measures based on global and temporal variations of dynamics in the *p*-space are proposed. A correlation is explored between the complexity measures derived from the *p*-space mapping of PPS that closely matches the cardiovascular state of a typical human subject.

The mathematical algorithms derived from a simple blood flow wave pattern can be easily applied for assessing other physiologic signals in the cardiovascular system obtained during perturbations caused by dynamic exercise, thermal stress, and potentially high terrestrial physiologic effects during hypobaric stress.

INTRODUCTION

Any periodic or nearly periodic signal can be characterized by three specific periodicity attributes or '*p*-attributes': the periodicity or period length, the repetitive wave-shape or pattern, and the multiplicative scaling factor associated with the successive periodic segments [7-9]. In case of dynamic, transitory physiologic signals, such as the blood pressure waveforms obtained from a finger plethysmograph, all three periodicity attributes may vary with time. In this report, several methods are proposed to analyze real-time dynamics of these three attributes of the signal both individually as well as collectively and to explore their relationship with the underlying cardiovascular state through a pilot study.

Multiple research studies on Heart Rate Variability (HRV) show that a healthy heart exhibits complex deterministic dynamics, whereas cardiac pathologies reflect in decreased complexity of the HRV signal: i.e. decreased cardiac chaos [1,4,12-14]. Conventional Fourier decomposition based analysis [1,4] assumes the signal being generated is from a linear process. Spectral analysis of HRV series reveals an inverse relationship between the spectral power and the frequency; such inverse or 1/f spectrum of HRV indicates its fractal or nonlinear nature [12]. Therefore, for the in-depth understanding of the cardiovascular process, nonlinear methods are routinely used [4,13,15], which is also the approach followed in the present work.

In HRV studies, only the variation in the 'periodicity' of ECG signal can be faithfully analysed. The present work attempts to study the cardiovascular dynamics through the analysis of the photo-plethysmographic signal obtained from a database that includes direct recordings from the finger (or digit). Many studies show that the digital blood volume pulsates in step with the human cardiac cycle, which is conveniently detected by the photo-plethysmograph [6,10,18]. The shape of the sensed pulsatile signal is similar to that of the intra-arterial blood pressure signal. Thus the HRV information is implicit with the photo-plethysmograph signal (henceforth called PPS); in addition, the wave-shape or pattern as well as the scaling or the magnitudes of the nearly repetitive segments of the signal are expected to reveal additional information on the cardiovascular dynamics. The proposed analysis in this report is a mathematical generic construct, obtained from data mining of multiple experimental studies [10] where information contained in all three periodicity attributes of an oscillatory time series is analyzed to assess the state of the underlying dynamics.

Hypothesis tested: Because the plethysmograph signal generally exhibits a certain degree of irregularity, there are two basic issues: (a) whether the irregularity in the signal is due to random variations in the underlying process or whether it is due to nonlinear determinism, and (b) in the latter case a particular focus is how the individual periodicity attributes influence the nonlinear determinism in the data. Conventionally, surrogate data analysis is used for the assessment of nonlinearity [17, 20]. Since there are certain caveats in the analysis of time series with strong periodic components through conventional surrogates [19,21], generation of a new class of mathematical surrogates is proposed, where the temporal order of the periodicity attributes are

randomized. These surrogate series retain the similar noisy limit cycle structure in the phase-space as the original series. The degree of determinism in the data is detected in the light of the generated surrogates, and the effect of the variations of individual attributes on the overall process is considered.

METHODS

To obtain a quantitative analysis of the dynamics associated with the collective variations of the three-periodicity attributes, a generic three-dimensional mapping scheme was designed where the coordinates were defined in terms of the individual periodicity attributes. Each periodic segment maps to one point in the proposed *p-space*. New complexity measures are proposed based on the static (or spatial) and the dynamic (or temporal) features of the formation of the cloud of points mapped from the signal. It is shown that the qualitative assessment of the underlying dynamics of the cardiovascular process is possible through the characterization of the mapping of the PPS series in the p-space.

Data recording used: In the original archival data set [10], a transmittance type photo-plethysmograph was used, where two series connected IR-LEDs operating at 3KHz are used as the source of light, and two phototransistors connected in parallel are used as the detectors. The optical components are fitted inside a finger-encircling cuff. The digital blood-volume pulsations, detected by the photo-transistors is passed through a 50 Hz notch filter followed by an amplifier and a 4^{th} order Butterworth filter with a cut-off at 40 Hz. The analogue output is digitised with 12-bit ADC. The data were recorded with a sampling frequency of 122 Hz. Segments of data free from motion artefacts are used for analysis.

Signal Decomposition: The relatively regular component is extracted from the plethysmograph signal as detailed in the following sections and shown in the RESULTS section in Figures 2(a) and 2(c) and Table 1 that depict a significant part of the extracted regular component of the plethysmograph signal.

Phase-space features: The phase-space diagrams of the plethysmograph signal and of its estimated regular component are presented in Figures 2(b) and 2(d) respectively.

PERIODICITY DETECTION AND DECOMPOSITION OF THE PLETHYSMOGRAPH SIGNAL

The typical plethysmograph signal contains one strong component with nearly repetitive pattern with a weak irregular residual component. In the present work, the signal is decomposed into these two components, which are separately analyzed. This decomposition involves: (i) the *detection* of the periodicity of the nearly repetitive component, and (ii) the *extraction* of the same from the composite signal. The general procedure for detection and extraction of nearly periodic segments feature are reviewed in references [7-9], and is summarized here; a modified scheme for estimation of the time varying periodicity is proposed in a later section.

Periodicity detection

Let the time series: $\{x(.)\} = \{x(1), x(2),...\}$ be configured into an mxN matrix A_N:

$$A_N = \begin{bmatrix} x(1) & x(2) & \dots & x(N) \\ x(N+1) & x(N+2) & \dots & x(2N) \\ \dots & \dots & \dots & \dots \\ x((m-1)N+1) & x((m-1)N+2) & \dots & x(mN) \end{bmatrix} \quad (1)$$

Singular value decomposition (SVD) [5,7] of any mxN matrix A_N is given by $A_N = \mathbf{USV}^T$, where $\mathbf{U} \in \mathbf{R}^{mxm}$ and $\mathbf{V} \in \mathbf{R}^{NxN}$ are orthogonal matrices, $\mathbf{S}$ ($\in \mathbf{R}^{mxN}$) = diag (s_1, s_2,..., s_r: **0**), r = min(m,N), $s_1 \geq s_2 \geq ... \geq s_r$. The number of nonzero singular values (s_i) gives the rank of A_N.

If $\{x(k)\}$ is *strictly periodic* (in repeating pattern and period length sense) with periodicity N (e.g., $x(k) = x(k+N)$), Rank(A_N) = 1. Again, if $\{x(k)\}$ is arranged into another matrix A_{iN} with row-length iN, i = any positive integer, Rank(A_{iN}) = 1. If $\{x(k)\}$ is *nearly periodic* with periodicity N, A_{iN} can be a full-rank matrix but the first singular value will be dominant (i.e. $s_1 >> s_2$). Thus, the presence of a dominant periodic component in any data sequence $\{x(k)\}$ will result in repetitive peaks (at multiples of the concerned period length N) in the s_1/s_2 vs. row length (n) spectrum, which is called the 'singular value ratio' (SVR)-spectrum [1,2] or the 'periodicity spectrum' [3] of $\{x(k)\}$; instead of s_1/s_2, any other rank-revealing index may also be used.

Periodic decomposition

The rank-1 approximation of the matrix $\mathbf{A}_N$, which also represents a periodic time series of periodicity N in $\{x(k)\}$, is given by $\mathbf{u}_1 s_1 \mathbf{v}_1^T$, where $\mathbf{u}_1$ and $\mathbf{v}_1$ are the first columns of **U** and **V** respectively. $\mathbf{v}_1^T$ represents the pattern over the periodic segments of the extracted component of periodicity N, while the successive elements of $\mathbf{u}_1 s_1$ are the scaling factors for the successive periodic segments. The residual component is given by the time series represented by the matrix $A_N - \mathbf{u}_1 s_1 \mathbf{v}_1^T$.

Analysis: $\mathbf{u}_1 s_1 \mathbf{v}_1^T$, the most dominant SV-decomposed component stands for the *best estimate* (in least squares sense) of the *periodic component of length N* present in $\{x(k)\}$; it is implicit that the *best estimate of the periodic pattern* is $\mathbf{v}_1^T$. The pattern estimation is completely adaptive, unlike alternative approaches; for example only sinusoidal components are permitted in Fourier decomposition based methods, and in wavelet transform [24] there is constraint as regards shapes or patterns of components.

Since, in real-life, the periodicity of $\{x(k)\}$ may vary with time, a moving data-window scheme [9] may be used for decomposition. If l_i be the periodicity in the i-th data window, the length of the (i+1)-th data window is ml_i, where $m \geq 4$ (as at least two peaks are necessary for periodicity detection in the p-spectrum). Two data windows (say i-th and (i+1)-th) thus overlap over (m-1)l_i data points. In i-th data window the prime periodicity l_i is detected using p-spectrum and the concerned periodic component is detected from which only the first period (of length l_i) is extracted; the procedure is repeated for the next data window. The so obtained successive periodic segments adjoined together constitute the estimated relatively 'regular' component $\{x(k)_{regular}\}$,

where the periodicity, as well as the pattern and the scaling factor may vary between the different segments.

Decomposition of the photo-plethysmograph signal (PPS)

Since the detection of the periodicity attributes is pivotal to the present study, the decomposition scheme stated above is further refined as follows. First, a fixed data window length (≥4 times the maximum expected period length) is considered. The periodicity within the data segment (say l_1) is detected using the p-spectrum and the corresponding periodic pattern is obtained. This pattern is linearly transformed by stretching or compressing to different period lengths (varying from $l_1/2$ to $3l_1/2$ for even l_1, and $(l_1-1)/2$ to $(3l_1+1)/2$ for odd l_1) and the correlation of each with the data segment of equal length from the beginning of the data window (both being normalized) is computed; the period length l_1^* for which the correlation is maximum is considered to be the period length of the first periodic segment within the data window. The data window is moved by the length l_1^* to form the next data window, on which the whole exercise is repeated.

Thus the first extracted periodic segment will have the normalized pattern $\boldsymbol{p}_1$, the period length l_1^*, and its scaling factor as (say) a_1. The corresponding error or residual vector $\boldsymbol{e}_1$ (= $(x(1), x(2), \ldots, x(l_1^*)) - \boldsymbol{p}_1(l_1^*)a_1$) is the first segment of the error component of {x(k)}. The successive $\boldsymbol{p}_1(l_1^*)a_1$ vectors and the corresponding $\boldsymbol{e}_i$ vectors respectively adjoined together make up the regular and the error (or the residual) parts of the signal respectively. The dynamics associated with the regular part in the plethysmograph signal through the individual p-attribute sequences: $\{\boldsymbol{p}_i\}$, $\{l_i^*\}$ and $\{a_i\}$ are then analyzed.

RESULTS

The nature of the periodicity and scaling sequence for a typical case (Case-2, Table 1) is depicted in Figures 1(a-b); the profile of the varying pattern (with each pattern normalized to a fixed period) for the same is shown in Figure 1(c). The plethysmograph signal and the phase-space plot for Case 1 is shown in Figures 2(a-b).

ASSESSMENT OF NONLINEARITY USING SURROGATE DATA

One of the key issues in the study of nearly periodic or apparently irregular physiological signals is to determine whether the underlying process is governed by low dimensional chaotic dynamics or by some non-deterministic rules. Some of the main constraints for such a study are the requirements of large number of data points and stationarity, as well as problems due to observational and dynamical noise etc., which can be potential sources of errors particularly in case of physiological signals [11,16,19]. So in the present context, a more modest goal is to demonstrate the nonlinearity associated with the signal rather than aiming to prove presence of chaos, as

nonlinearity is a necessary condition for the presence of low dimensional chaos. This has given rise to the popular surrogate analysis [17,20] (discussed in the next section), which has been used and modified in the present study.

The detection of nonlinearity being the objective, a null hypothesis of the data being generated by certain static transformation of a linear stochastic process is considered (because the simplest type of nonlinearity in the data will at least be akin to static nonlinear transformation generating nongaussian output for a stochastic input series with Gaussian distribution). Corresponding to the data series, the surrogate data are generated, which are sets of random data having the same power spectrum and the same temporal amplitude distribution as the original series. To test the null hypothesis, the original series and the surrogate series are subjected to a procedure sensitive to nonlinearity, and a discriminating statistic is considered; the rejection of the null hypothesis amounts to the detection of nonlinearity.

In the Iterative Amplitude Adjusted Fourier Transform (AAFT) surrogate generator [17], close match with the original data both with respect to the *power spectrum* $\{X_k^2\}$ as well as the *amplitude rank distribution* $(\boldsymbol{o}_x)$ is achieved by which $\{x(k)\}$ is shuffled randomly $\{x_k^{(0)}\}$, subsequently followed by a two stage iterative procedure:

(i) The power spectrum of $\{x_k^{(i)}\}$ is replaced by $\{X_k^2\}$, and

(ii) the reverse transformed series is rank ordered to $(\boldsymbol{o}_x)$. The proposed surrogate generators incorporate the AAFT approach.

The Fourier transformation based surrogate generation schemes discussed above are nonparametric and are concerned with a linear null hypothesis. Although this type of surrogate analysis is routinely employed for the analysis of nonlinear time series, there can be problems in case of periodic processes (or for systems with long coherence time) [19, 21]. Strong nearly periodic rhythms are explicit in the present plethysmograph signal (Figures. 2(a), 2(c)). Ideally, the surrogate of such a nearly periodic time series should be another periodic time series [23]. In other words, if the original time series exhibits a limit-cycle behaviour in phase-space, surrogate data should also correspond to similar limit cycle. On the other hand, a time series producing noisy limit cycles (Figures 2(b) and 2(d)) is not generated by a linear stochastic process, even if observed through a static monotonic nonlinear transformation. A partial solution to this problem was addressed in [22], where the hypothesis of temporal correlation between successive nearly periodic segments was tested; the surrogate was generated by shuffling the sequence of complete cycles, disregarding the individual characteristic periodicity attributes of the cyclical segments, thus retaining the mutual coupling between the three periodicity attributes.

In the present context, the regular component of the signal exhibits variations in all three periodicity attributes (shown in Figure 1). Since the interest in this report lies in understanding the influence of the individual *p*-attributes on the overall dynamics, a new class of surrogate generators is proposed next, which preserves the limit cycle structure of the original time series.

Proposed surrogates

Three different surrogates are generated by the randomization of the three periodicity attributes as follows.

Preparatory steps:

(i) Decomposition:

The original signal is decomposed as $\{x(k)\} = \{x(k)_{regular})\} + \{x(k)_{residual})\}$ with

$$\{x(k)_{regular})\} = \{\boldsymbol{p}_1(l_1)a_1 : \boldsymbol{p}_2(l_2)a_2 : \ldots : \boldsymbol{p}_n(l_n)a_n\}, \quad (2)$$

where n is the number of contiguous periodic segments extracted from the signal; each periodic segment is characterized by its own periodicity or period length l_i, periodic pattern $\boldsymbol{p}_i$ and scaling factor a_i. The global pattern ($\boldsymbol{p}_g$) is obtained by averaging the $\boldsymbol{p}_i$ vectors defaulted to the same period length. ($\{X_k^2\}$) is the power spectra of $\{x(k)_{regular})\}$.

Analysis: Here the pattern $\boldsymbol{p}_i$ is considered to define a normalized profile; the normalization is with respect to period-length. The periodicity, the pattern and the scaling factor are algebraically independent entities.

(ii) Rank-ordering: Within the individual surrogate generators, the periodicity sequence $\{l_i\}$ and the scaling factor sequence $\{a_i\}$ are ordered according to the amplitude ranking, while the sequence of normalized pattern segments $\{\boldsymbol{p}_i\}$ is sorted according to the correlation ($\boldsymbol{p}_i^T \boldsymbol{p}_g$) of the segments against the global pattern. The order of ranking with respect to the individual attributes in the respective sequences (say, $\mathbf{o}_l$, $\mathbf{o}_p$, $\mathbf{o}_a$ respectively) is noted.

Generation of the surrogates:

(A) Surrogate generation through randomization of the period-length or 'periodicity' attribute: The periodicity sequence $\{l_i\}$ (i.e. $\{l_1, l_2 \ldots, l_n\}$) is randomly shuffled to $\{l_i\tilde{}\}$ keeping the associated scaling and pattern features unchanged; the patterns $\boldsymbol{p}_i$ are linearly stretched or compressed as necessary. The resulting time series $\{\boldsymbol{p}_1(l_1\tilde{})a_1 : \boldsymbol{p}_2(l_2\tilde{})a_2 : \ldots : \boldsymbol{p}_n(l_n\tilde{})a_n\}$ is Fourier transformed, the power spectrum is replaced with ($\{X_k^2\}$), and reverse Fourier transform is performed; the successive cyclical or periodic segments of the resulting time series are rearranged to conform to $\mathbf{o}_l$. As this reordering tends to disturb the power spectrum, the procedure is iterated twice, which produces closer match with ($\{X_k^2\}$, $\mathbf{o}_l$), resulting in the periodicity shuffled surrogate. The null hypothesis to be tested with this surrogate is that all the information lies in the pattern and scaling, while the periodicity factor does not contribute to the dynamics of the series.

(B) Surrogate generation through randomization of the 'pattern' attribute: $\{\boldsymbol{p}_i\}$ is scrambled to $\{\boldsymbol{p}_i\tilde{}\}$, while the other two attributes are left unchanged, generating the series $\{\boldsymbol{p}_1\tilde{}(l_1)a_1 : \boldsymbol{p}_2\tilde{}(l_2)a_2 : \ldots : \boldsymbol{p}_n\tilde{}(l_n)a_n\}$, which is Fourier transformed. The same way as above, the power spectrum is replaced with ($\{X_k^2\}$), and reverse transform is performed. The successive nearly periodic segments are reordered as per $\mathbf{o}_p$ sequence, and the whole procedure is repeated twice, leading to the pattern shuffled surrogate. Here the null hypothesis to be tested that all the information lies in the periodicity and the scaling, while the pattern variation does not contribute to the overall structure of the series.

(C) Surrogate generation through randomization of the 'scaling' attribute: The sequence $\{a_i\}$ is randomized to $\{a_i^{\sim}\}$, generating the time series $\{\boldsymbol{p}_1(l_1)a_1^{\sim}: \boldsymbol{p}_2(l_2)a_2^{\sim}:\ldots: \boldsymbol{p}_n(l_n)a_n^{\sim}\}$. Its power spectrum is replaced with $(\{X_k^2\})$, and the scaling factors of the successive periodic segments of the reverse transformed series are reordered as per $\mathbf{o}_a$ sequence, and the whole procedure is repeated twice, leading to the scaling factor shuffled surrogate. Here, the null hypothesis is that the scaling sequence does not govern the dynamics and the entire information lie in the pattern and periodicity variations.

Analysis: (i) Conventional surrogates have an inherent tendency towards statistical Type I error (i.e. the false rejection of null hypothesis) for the analysis of signals with long coherence time (or oscillatory series) due to the distortion of the phase space structure; these new surrogates are proposed to alleviate this problem by preserving the phase space geometry qualitatively.

(ii) For the analysis of the residual component $\{(x(k)-x(k)_{regular})\}$, which is devoid of oscillatory structure, the conventional AAFT surrogate generator [20] is employed.

Detection of determinism

Detection of determinism by conventional means can be problematic in case of lack of stationarity, noise contaminations, availability of limited amounts of data etc. as discussed earlier. In the present work, a method based on nonlinearly scaled singular value distributions has been used [2,3]; a broad outline of the method follows.

The data series $\{x(k)\}$ and its surrogate $\{x_{surr}(k)\}$ are configured into different mxn matrices $\mathbf{A}$ and $\mathbf{A}_{surr}$ with varying n. The scaled distributions of the respective singular values are generated and are analyzed for characterization of the process as follows. The total energy in $\mathbf{A}$ $(=\{\{a_{ij}\}\})$, given by $\Sigma_i\Sigma_j\, a_{ij}^2 = \Sigma_i\, s_i^2$ (i = 1 to rank($\mathbf{A}$)), is normalized for each configuration $\mathbf{A}$, preserving the Frobenius norm. Since rank($\mathbf{A}$) will be different for different n, a value R close (not a limitation) to the minimum rank($\mathbf{A}$) is chosen. For each n, the total energy $\mathbf{A}$ is linearly mapped to R normalized singular values. Thus for M different values of row length n, M sets of R singular values are obtained from which the mean singular values $s_m(i)$, (i = 1 to R) are computed. The scaled distribution $i^2 s_m(i)$ is plotted against i for i = 1 to R, for both $\{x(k)\}$ and $\{x_{surr}(k)\}$. The sets of distributions of the singular values with varying n are nonlinearly related; this is over and above the nonlinear weighting of the distributions within each set.

The discriminating features between the deterministic and stochastic processes reflected in the distribution of the nonprime singular values. For a purely stochastic series, all the singular values being isotropically distributed, $i^2 s_m(i)$ will be gradually increasing tending to saturate at a high value, since the singular values are arranged in a non-increasing order. On the other hand, for a series, with increasing i, the singular values s_i will be having significantly decreasing magnitudes tending to be vanishingly small, and hence $i^2 s_m(i)$ will be eventually decreasing tending to saturate at a low value. The distributions of $i^2 s_m(i)$ against i (bet. 1 to R) for $\{x(k)\}$ and $\{x_{surr}(k)\}$ are compared using Mann-Whitney (M-W) rank-sum statistic (Z) [25]. This is normally distributed with zero mean and unit variance, under the null hypothesis that the two observed samples came from the same distributions. If $|Z|>1.96$, the associated null hypothesis can be rejected with greater than 95% confidence level [25].

Each kind of the surrogates is used to assess the determinism in the regular component in the above way by computing the M-W rank-sum statistic ($|Z_I|$ for periodicity shuffled surrogate, $|Z_p|$ for pattern shuffled surrogate and $|Z_a|$ for scaling factor shuffled surrogate). For the detection of determinism in the residual component, the corresponding Z-value ($|Z_{res}|$) is computed using AAFT surrogate the same way.

Proposed *p*-attribute map and complexity measures

***p*-attribute *space* and map:** The three attributes, the periodicity, the periodic pattern and the scaling factor, are independent entities, and collectively the three can precisely define a periodic segment. Hence a novel 3-dimensional space is constructed, where the *periodicity* and the *scaling factor*, both normalized, act as two coordinates, while the *pattern correlation* acts as the third coordinate; the pattern correlation is given by the correlation of the wave-shape or pattern of a segment with respect to the global pattern. The *p*-attribute sequences extracted from a nearly periodic series can be mapped into the proposed space, which we call *p*-attribute *space* or simply *p-space*. A point in this space represents one periodic segment of the regular component of the nearly periodic signal. The sequence of periodic segments mapped into the p-space, called the p-attribute map, portrays the complete dynamics of the regular component. The trajectory joining these points sequentially depicts the temporal evolution of the process in the *p*-space.

Analysis: (i) Any *strictly periodic* process (whether sinusoidal or not) is represented by *a single point* in the *p*-space, which shows the minimal dynamical variations. (ii) The *p*-space mapping assumes a global pattern to be available.

Characterization of the dynamics through the distribution in *p*-attribute *space*

Reference point: A reference point is first considered within the p-space, which represents a state of minimum dynamics for a cyclical process, i.e. a process which is strictly periodic. The implication is that the reference point lies on the plane with pattern correlation as unity. The mostly occurring periodicity, called the 'modal periodicity', is chosen as the periodicity coordinate of the reference point. The scaling factor usually being a random phenomenon, the average value of the scaling factors for the process studied is considered as the concerned scaling co-ordinate for the reference point. The following two complexity measures quantify spatial and temporal evolution of the cyclical process.

Spatial Complexity Measure C_s: In the three-dimensional p-space, the distance between the nearest point and the furthest point of the map from the reference point is considered as the range of the map, which is divided into n^* spherical sections of equal width (e.g. if the smallest sphere is of outer radius r, the outmost spherical shell has the outer radius of n^*r). The fraction of the total number of points in each section of the map, i.e. the fraction of points in each spherical shell centred on the reference point, is computed. Higher fraction of points being close to the reference point (i.e. the clustering around reference point) indicates the tendency of less variation of the *p*-attributes.

The spatial *p*-map dynamics is indicated by the measure:

$C_s = \Sigma i\, f(i)$,

where $f(i)$, i=1,2,..., n^* is the distribution of points, and i is the section index; in the present case n^* is considered as 10 (which is not a limitation). Thus C_s is a spatial distribution index, which measures the degree of deviation of the global dynamics from a strictly periodic process. The higher the value of C_s, the higher is the variation measured globally. However, C_s is independent of the temporal ordering of the successive cyclical segments, for which a separate index (C_d) is proposed.

As the pattern correlation is confined to values ≤1, whereas the other two coordinates-values lie on either side of the reference-point, it is a semi-spherical space within which the mapped points lie. The volume of the j-th shell being $(3j^2 - 3j + 1)/2$ times the first one, the present mapping over-weights the j-th shell $j(3j^2 - 3j + 1)/2$ times, as higher dynamics is associated with the points lying in outer shells.

Temporal Complexity Measure C_d: The dynamic measure (C_d) is defined as the mean distance moved between successive points in the p-space. A higher value of C_d indicates higher dynamics. Unlike C_s, which is a static measure, C_d is a complementary measure of temporal evolution of the process into the cloud of points in the p-space. In the present context, C_d indicates the beat-to-beat variability of the plethysmograph signal.

Analysis: (i) By hypothesis, clustering around a point in the *p-space* away from the reference point and more dominant than the cluster around the reference is not possible, as that would mean mostly one repetitive profile being dominant, which would in fact be the reference point profile. (ii) As the points move away from the reference point in the p-space, their pattern correlations decrease from 1 to a lower value, while the periodicity and the scaling co-ordinates lie on both sides of the reference point values.

Case Study Analyses

Raw data derived from previous legacy studies [10] from six different cases showing wide medical histories are analyzed to validate the above mathematical routines. The results are summarized in Table 1 and Figures 2, 3 and 4.

Table 1. Summary of case studies from archival database [10].

Cases	Medical History of subject	Energy in residual component	Determinism assessment indices				*p*-map complexity indices	
			$\|Z_l\|$	$\|Z_p\|$	$\|Z_a\|$	$\|Z_{res}\|$	C_S	C_D
1	Postoperative (thoractomy) clinically stable subject in ICU. Age: 64.	1.8%	2.90	5.20	1.57	1.77	4.00	0.30
2	Quasi-stable case following hernia and cardio-thoracic surgery, in ICU, hypotensive. Age: 69.	2.7%	0.65	2.96	1.39	2.18	1.38	0.14
3	Subject with hypoxic brain damage following road accident, unstable, in ICU, with right hemiphlegia. Age: 27.	8.1%	0.31	0.35	1.73	2.26	1.76	0.21
4	Oral chemotherapy, operated for breast cancer, BP normal. No cardiac problem. Age: 57.	1.5%	3.41	3.39	1.94	1.83	3.22	0.42
5	Angina , high BP for 17 years. Age: 65.	3.2%	2.22	2.88	1.26	0.01	2.32	0.20
6	Suffered a stroke 5 years back. one defective heart valve, hypotensive. Age: 68.	2.7%	2.44	2.72	1.76	1.30	2.30	0.24

C_d tracks the beat-to-beat variability of the plethysmograph signal.

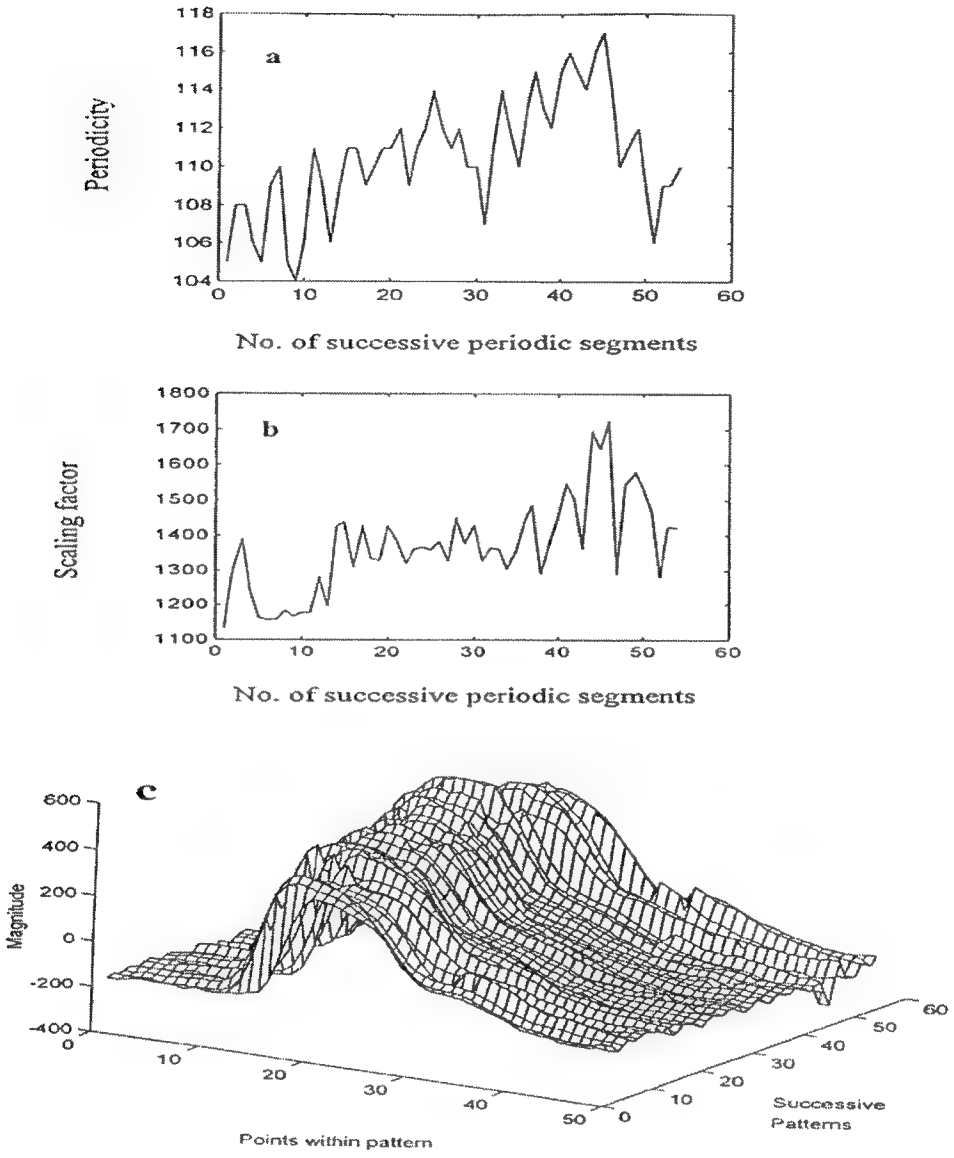

Figure 1. (a) The variations in the periodicity over a segment of data in Case-2, (b) the corresponding variations of the scaling factor, (c) the varying pattern profiles of the successive periodic segments with the periodic length defaulted to a fixed value.

Figure 2. (A)-(b) The photo-plethysmograph signal for a post-operative stable patient (case-1 in table 1), and its phase-space plot. (c)-(d) the regular component extracted from the signal (a), and the corresponding phase-space plot. (e)-(f) the aaft surrogate series generated from (c), and the corresponding phase-space plot. (g)-(h) the surrogate generated by shuffling the scaling factors and the corresponding phase-space plot. (i)-(j) the surrogate generated by shuffling the

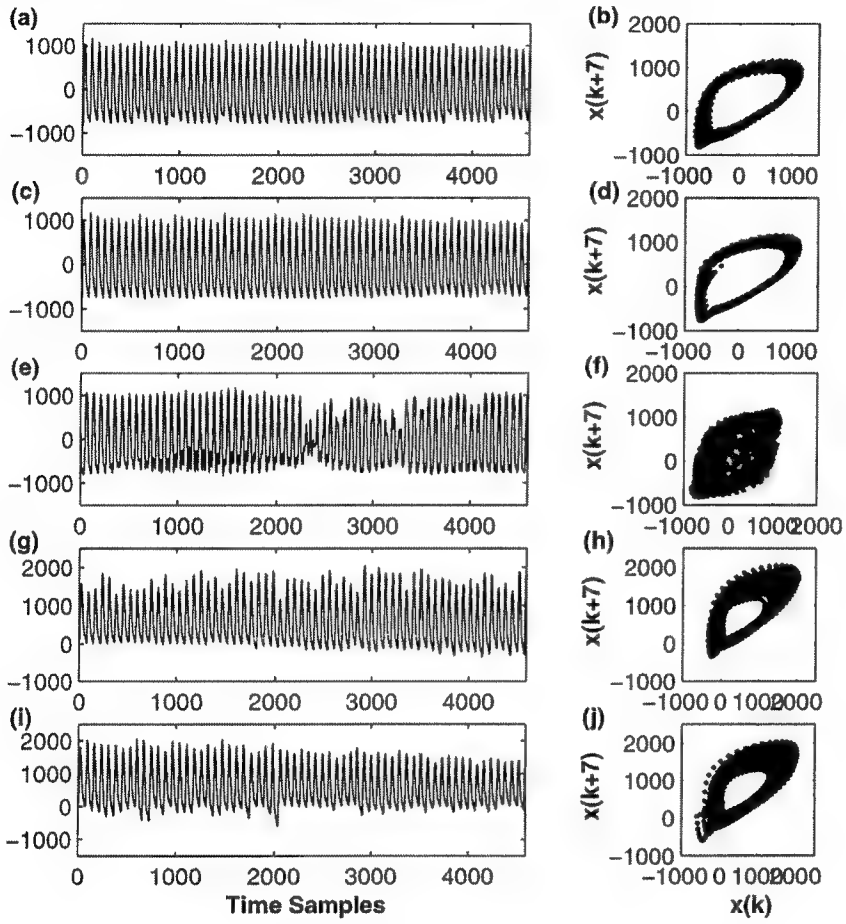

patterns of the periodic segments and the corresponding phase-space plot. Note that in both (h) and (j) the noisy limit cycle structure is retained, whereas in (f) it is destroyed.

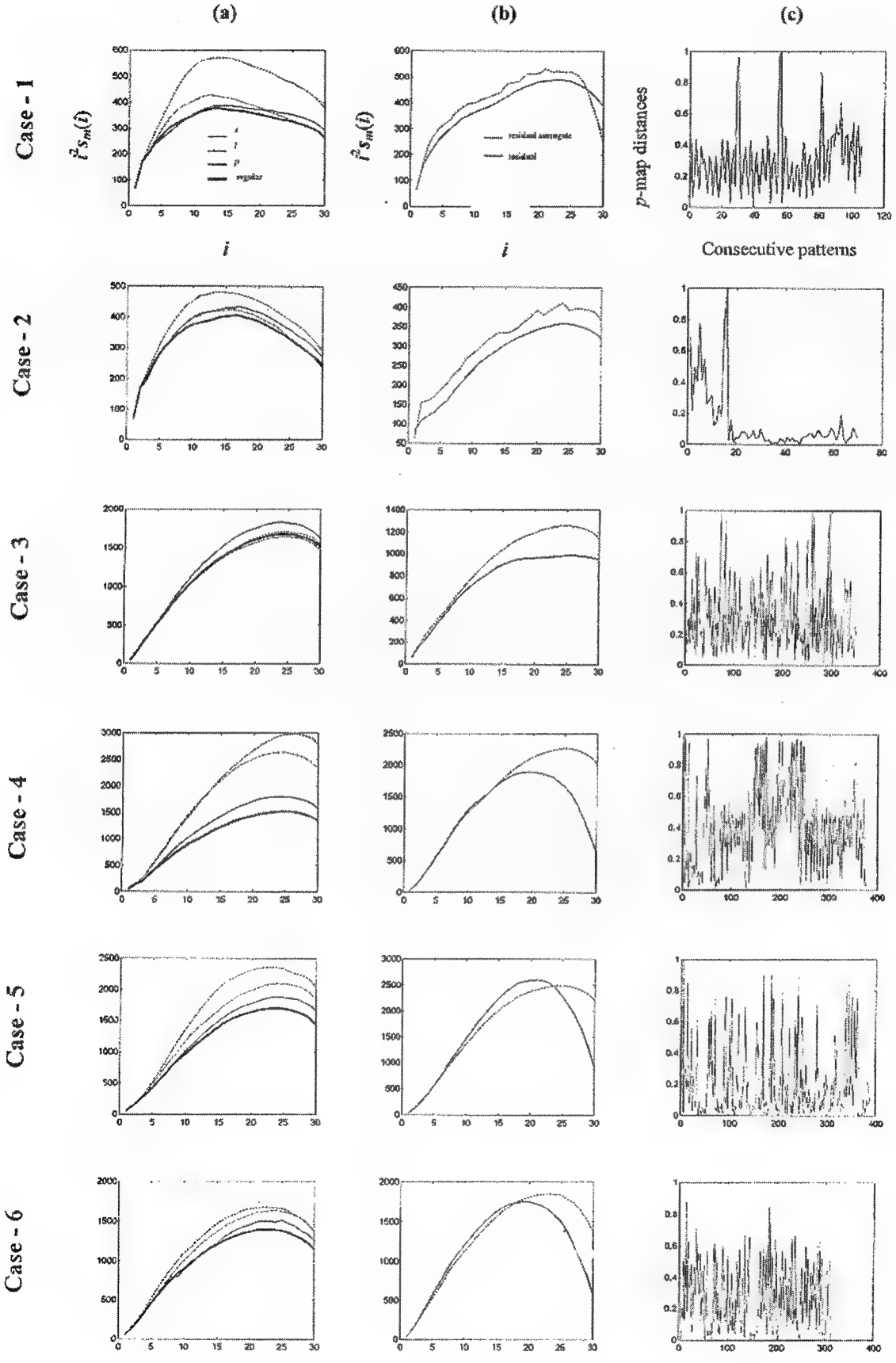
(a)
(b)
(c)
Case - 1
Case - 2
Case - 3
Case - 4
Case - 5
Case - 6
$i^2 s_m(i)$
$i^2 s_{\bar{m}}(i)$
p-map distances
i
i
Consecutive patterns
residual surrogate
residual
regular

Figure 3. Column (a): The scaled singular value distribution (($i^2 s_m(i)$) of the regular component against the same for the surrogates generated through the shuffling of the periodicity, the pattern and the scaling sequences for Case-1 to Case-6.
Column (b): The scaled singular value distribution of the residual component against the AAFT surrogates for Case-1 to Case-6.
Column (C): Profiles of the distances between successive points in the *p*-map for Case-1 to Case-6.

Figure 4. Fraction of points in successive shells centred around the reference point in the *p*-map for Case-1 to Case-6.

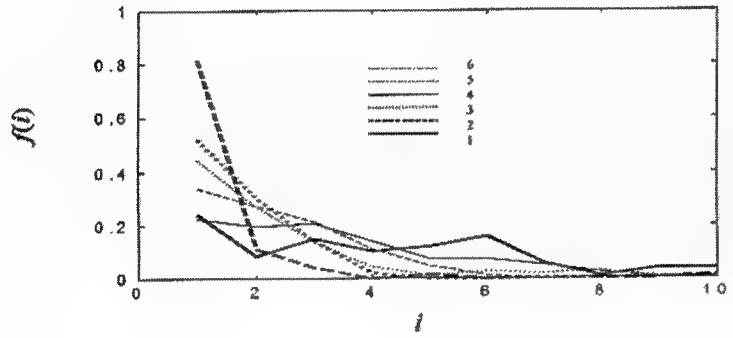

The above figures indicate that the extracted component derived by the specific mathematical routines has essentially captured the dynamics of the raw data macroscopically. Additionally, the time series of AAFT surrogate of the estimated data, and the phase-space plot are shown in Figures 2(e)-(f). From the visual inspection it appears that the surrogate series possesses different dynamics compared to the original signal. The phase-space plot shows that the *noisy limit cycle structure is completely destroyed*. The time series and their phase-space plot of the proposed nonlinear surrogates with randomized scaling and periodicity and pattern sequences are displayed in Figures 2(g)-(l), retaining the noisy limit cycle structure.

Assessment of determinism: From the present analysis, the following observations emerge:

(a) Pattern variations: For healthy subjects with normal cardiac states (Case-1, Case-4) there is distinct determinism in the plethysmograph signal due to pattern variations; the $|Z_p|$ values are found to decrease from a high value (e.g., 5.2 in Case-1 and 3.39 in Case-4) to lower values with increasing instability (e.g., in Cases 2, 5 and 6) implying low determinism. In Case-3 which is an unstable case, stochasticity in the signal due to pattern variation is reflected in the $|Z_p|$ value (<1.96).

(b) Periodicity variations: Nearly similar behavior for periodicity variation is observed from the $|Z_l|$ values. This implies that the periodicity variation affects the determinism in the signal in the same way as the pattern variation.

(c) Scaling variations: The influence of the scaling variations are consistently of the stochastic nature as $|Z_a|$<1.96 in all cases. This implies lack of information regarding cardiovascular stability in the variation of the scaling factors.

(d) Study of the residual series: Within Cases 1-4, with increasing instability $|Z_{res}|$ tends to increase from stochastic region to deterministic domain with low degree of determinism. For Cases 5 and 6 the scaled singular value profiles of the residual and the surrogate (Figures 2 (b)) tend to cross over significant regions leading to low $|Z_{res}|$ values though the concerned cardiovascular states are disturbed. So no conclusive results emerge from the study of the residual.

p-map dynamics: The *p*-map dynamics, which provide a collective picture of the *p*-attribute variations, alternatively uniquely reflect the relative state of cardiovascular stability.

(a)The C_s measures obtained from the distribution of points around the reference point in the *p*-map (Figure 4) are high (implying higher dynamics) for stable cases (e.g., 4.0 and 3.22 in Case 1 and 4 respectively) and fall to lower values with increasing instability.

(b)The C_d measures, which indicate the mean of successive distances covered (Figure 2(c)) in the *p*-map also show similar distinctive behavior as C_s, being relatively high (0.3 and 0.42 for cases 1 and 4 respectively) for stable cases and low for pathological cases.

Analysis 1: Due to the variations in the BP pulse propagation delay (also known as Pulse Transit Time (PTT)), which is a function of the elastic properties of the arterial wall between the left ventricle and the periphery (i.e. the finger), the variability of the cardiac periodicity detected through the plethysmograph signal will be different from the conventional HRV sequence generally computed from R-R intervals of ECG complexes. This together with the fact that change in the length of the cardiac cycle can influence the diastolic decay and thereby change the wave-pattern, the proposed assessment of cardiovascular state through the periodicity attributes of the plethysmographic signal can be more informative than the HRV studies. The present findings of decreased complexity in case of cardiac pathologies conform to those from HRV studies [5-8].

CONCLUSIONS

A generic mathematical algorithm process for analyzing complex physiologic signals in terms of the time-varying periodicity attributes, typically derived from techniques such as digital plethysmography, has been presented. First, the complex waveform determinism is detected through scaled singular value distributions of the signal against three specific classes of surrogates generated from the three periodicity attributes. These surrogates, generated by randomizing the mutual associations between the different *p*-attributes, are shown to preserve stable noisy limit-cycle structure in the phase-space.

The results of a validation of blood wave patterns obtained from an archival database show that the signal dynamics associated with the periodicity attributes contain meaningful relationship with the condition of the underlying process. While the effect of the scaling factor is largely stochastic in nature, the degree of determinism in the signal due to the pattern and the periodicity variations is observed to be highly correlated with relative chaotic function of the cardiovascular state of a given human subject; with the degree of determinism tending to decrease with increasing instability.

The effects of the variations in the *p*-attributes have also been collectively analyzed through the proposed mapping in three-dimensional *p*-space; one unique feature of this mapping is that one periodic segment is described by one point in *p*-space. The present report verifies that the cardiovascular status is consistently reflected in the distribution of points in the *p*-map around the reference point. As reflected in both the static and the dynamical measures of complexity, the distribution of points in the p-space is more spread out in stable, healthy subject cases representing higher variations in the underlying dynamics, while it tends to be heavily clustered close to the reference point in pathological or unstable human subject cases indicating the loss of complexity (decreased chaos) as implied from other studies [15].

Application of this mathematical algorithm technique can be reasonably, and easily, employed to derive and separate complex wave patterns affecting cardiovascular status during various perturbations of the physiological system.

REFERENCES

1. Akselrod S., D.Gordon, F.A.Ubel, D.C.Shannon, A.C.Berger, and R.J. Cohen. Power spectrum analysis of heart rate fluctuations: a quantitative probe of beat-to-beat cardiovascular control. *Science.* 213: 220-222,1981.

2. Bhattacharya J., and P.P.Kanjilal. On the detection of determinism in a time series *Physica D.* 132, 100-110,1999.

3. Bhattacharya J., and P.P.Kanjilal. Assessing determinism in photo-plethysmographic signal, *IEEE Trans. Syst. Man Cybernetics* Pt. A 29, 406-410,1999.

4. Cerutti S., S. Baselli,A.N. Bianchi, L.T. Mainardi, M.G. Signorini, and A.Malliani. Cardio-vascular variability signals: From signal processing to modelling complex physiological interactions. *Automedica.*16, 45-69,1995.

5. Golub G., and C.F.Van Loan. Matrix Computations. 3rd Ed., The Johns Hopkins Univ. Press, Baltimore, 1996.

6. Hertzman A. B. The blood supply of various skin areas as estimated by the photoelectric plethysmograph, *Amer. J. Physiol.*124:328-340,1938.

7. Kanjilal P.P. Adaptive Predictions and Predictive Control Peter Peregrinus Ltd., Stevenage, UK, 1995.

8. Kanjilal P.P.,S.Palit , and G. Saha. Fetal ECG extraction from single-channel maternal ECG using singular value decomposition, *IEEE Trans. Biomed. Engr.* 44, 51-59,1997.

9. Kanjilal P.P.,J.Bhattacharya, and G. Saha. Robust method for periodicity detection and characterization of irregular cyclical series in terms of embedded periodic components. *Physical Rev.* 59: 4013-4025,1999.

10. Kanjilal, P.P., J. Bhattacharya, V. Muralidhar, and H.L. Kaul. An instrument for non-invasive continuous measurement of blood pressure using a finger cuff. *J. Anaesthe. Clin. Pharmacol.* 13: 283-289,1997.

11. Kantz, H., and T. Schreiber. Dimension estimates and physiological data. *Chaos.*5:143-154, 1995.

12. Kobayashi, M., and T. Musha 1/f fluctuation of heartbeat period. *IEEE Trans. Biomed. Engr.* 29:456-457,1982.

13. Kurths J., A. Voss,P. Saparin, A.Witt, H.J.Kleiner, and N.Wessel. Quantitative analysis of heart rate variability. *Chaos.* 5:88-94,1995.

14. Malik, M., A.J.Camm. *Heart Rate Variability*, Futura Publishing Co., Inc., Armonk, NY.1995.

15. Poon C.-S., and C.K. Merrill. Decrease of cardiac chaos in congestive heart failure. *Nature.* 389:492-495,1997.

16. Rapp, P.E. Chaos in neurosciences, cautionary tales from the frontier. *Biologist.* 40:486-491,1993.

17. Schreiber T., and A.Schmitz. Improved surrogate data for nonlinearity tests. *Physical Review Letters.* 77:635-638,1996.

18. Sherebin M.H. and R.Z. Sherebin. Frequency analysis of peripheral pulse wave detected in the finger with a photoplethysmograph. *IEEE Trans. Biomed. Eng.* 37: 313-317,1990.

19. Stam, C.J., J.P.M. Pijn, and D.M. Pritchard. Reliable detection of nonlinearity in experimental time series with strong periodic components. *Physica.*112:361-380,1998.

20. Theiler J., S.Eubank, A.Longtin, B. Galdrikian, and J.D.Farmer. Testing for nonlinearity in time-series:the method of surrogate data. *Physica.*58:77-94,1992.

21. Theiler, J., P.S.Linsay, and D.M. Rubin. Detecting nonlinearity in data with long coherence times. in A.S. Weiegend, and N. Gershenfeld (Eds), *Time Series Prediction, Forecasting the Future and Understanding the Past.* Addison Wesley, Reading, MA, 1993.

22. Theiler, J. On the evidence of low-dimensional chaos in an epileptic encephalogram, *Phys. Letts.* 196:335-341,1995.

23. Theiler, J., and P.E.Rapp. Re-examination of the evidence for low dimensional nonlinear structure in the human electroencephalogram. *Electroencephal. Clin. Neurophysiol.* 98: 213-222,1996.

24. Wickerhauser, M.V. *Adapted Wavelet Analysis from Theory to Software.* AK Peters, Wellesley, MA, 1994.

25. Zar J.H., *Biostatistical Analysis.*2nd Ed., Prentice Hall, NJ, 1984.